

Cooling Configuration Effect on the Thermal Risk of Tubular Reactor

Lamiae Vernieres-Hassimi^{*a}, Valeria Casson-Moreno^b, Moulay-Ahmed Abdelghani-Idrissi^a, Sébastien Leveneur^{a,c}

^a Normandie Univ, INSA Rouen, UNIROUEN, LSPC, EA4704, 76000 Rouen, France.

^b University of Bologna/UNIBO Department of Civil, Chemical, Environmental and Materials Engineering

^c Laboratory of Industrial Chemistry and Reaction Engineering, Johan Gadolin Process Chemistry Centre, Åbo Akademi University, Biskopsgatan 8, FI-20500 Åbo/Turku, Finland.

lamiae.vernieres@insa-rouen.fr

Maximum temperature of reactant mixture is an important parameter regarding reactor safety. If the control of reaction temperature is lost, then side or decomposition reactions may be triggered leading to thermal runaway situation. This study concerns a liquid phase reaction system. This paper explores the influence of parameters on the thermal safety of a pilot tubular reactor. The following parameters were studied: the inlet temperature of the coolant, the volumetric flow rate, and the co-current flow and the counter-current flow configurations. The aim was to identify the main parameters that control the reaction temperature in the presence of a fast exothermic reaction system. The results showed that co-current configuration allows to control the maximum temperature. By changing the configuration, the cooling power can be reduced compared to a change in the inlet temperature of the coolant. A criterion of stability has been implicated in order to confirm this result.

1. Introduction

Chemical reactors are usually the heart of chemical processes, because it is where chemical reactions occur and produce the desired chemicals. Chemical engineers should determine the best operating conditions to optimize the yield of a product by limiting the waste and avoiding the trigger of thermal runaway. When some exothermic chemical processes are at stake, one or several dysfunctions, e.g., cooling failure or wrong operating conditions, can lead to an increase of heat-flow rate due to chemical reactions compared to the absorbed heat-flow rate. Then, the resulting temperature increase can cause decomposition of chemical compounds leading to an overpressure in the reactor and an explosion (Leveneur et al. 2016). A recent study carried out by (Saada et al. 2015) has shown that thermal runaway accidents are still significant. (Dakkoune et al. 2018) observed that 25% of the major accidents in chemical industries are due to runaways. Despite the fact that much progress has been made to understand and limit such runaway reactions, this problem still occurs. According to reference (Westerterp and Molga, 2006), three lines of defence have to be considered to prevent a reactor accident: the choice of right operating conditions, (Maestri and Rota, 2016); an early detection and warning system, (Guo et al. 2016); a suitable system to handle thermal runaway, (Torré et al. 2008). In the literature, there are several articles dealing with thermal process safety assessment for batch or semi-batch reactor (Casson et al. 2014), but the articles dedicated to the process safety of continuous process are relatively scarce (Vernières-Hassimi and Leveneur, 2015). The aim of this work is to study the influence of coolant on the maximum temperature. The following parameters were studied: the coolant inlet temperature, the volumetric flow rate, and the co-current flow and the counter-current flow configurations. Many studies have been done in recent decades on the advantages and disadvantages of counter-current and co-current cooling configurations for example (Luss and Medellin, 1972), (De Morais et al. 2004). However any of these authors proposed a stability criterion for PFRs, in literature, several thermal stability criteria specifically created for PFRs exist (Copelli, 2016). In the present work we apply to our experimental data the criterion formulated by (Dente and Collina, 1964), that historically was the first reactor stability criteria created ad hoc for tubular

reactors. The reaction chosen for this study is sodium thiosulfate oxidation by hydrogen peroxide, which is a very exothermic reaction with fast kinetics (Cohen and Spencer, 1962), (Lo and Cholette, 1972), (Brungs et al. 1988). This reaction system is considered as a model for chemical reactors engineering studies (Grau et al. 2002),

2. Experimental

Figure 1 illustrates the double-jacketed tubular chemical reactor, represented by an assembly of 10 modules. Each module is 0.8 m in long. The mixture reactant was pumped into the inner glass tube, while the cooling fluid circulates in a counter-current or co-current configuration through the outer glass tube. Temperature sensors were placed at the inlet and outlet of each module. The geometrical and physical parameters of the tubular reactor can be found in the previous articles of our group (Vernières-Hassimi et al. 2015). The geometrical and physical parameters of the tubular reactor are indicated in Table 1.

Table 1: Geometrical and physical parameters of the tubular reactor

| | geometrical parameters | | | physical parameters | | |
|------------|-------------------------|-------------------------|------|--|--|-------------------------|
| | D (m) | e _w (m) | L(m) | λ (W.m ⁻¹ K ⁻¹) | C _p (J.kg ⁻¹ K ⁻¹) | ρ (kg.m ⁻³) |
| Inner pipe | 1.84 x 10 ⁻² | 1.80 x 10 ⁻³ | 8.63 | 1.2 | 380 | 2200 |
| Outer pipe | 3 x 10 ⁻² | 2 x 10 ⁻³ | 8.63 | 1.2 | 380 | 2200 |

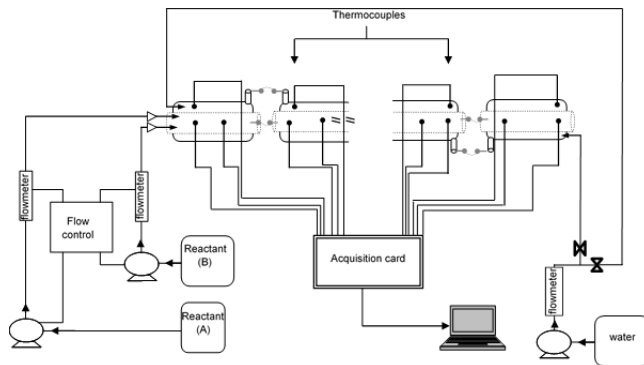
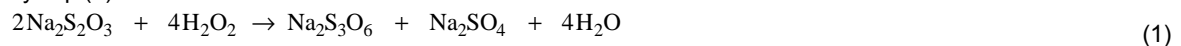


Figure 1: Experimental set-up of the tubular reactor.

3. Mathematical modelling

When the ratio of hydrogen peroxide concentration (C_A) to sodium thiosulfate concentration (C_B) is higher than or equal to 1.96 (Cohen and Spencer, 1962), the oxidation of sodium thiosulfate by hydrogen peroxide is given by Eq. (1).



The reaction kinetics for sodium thiosulfate is given by Eq. (2).

$$r = A_0 \exp\left(-\frac{E}{RT_r}\right) C_A^\alpha C_B^\beta \quad (2)$$

In this study, the kinetic parameters and reaction enthalpy ΔH determined by (Aimé, 1991) were used:

$$\alpha=1.5; \beta=0.6; A_0=6.75 \cdot 10^8 \text{ m}^{3.3} \cdot \text{mol}^{1.1} \cdot \text{s}^{-1}; E=80256 \text{ J} \cdot \text{mol}^{-1} \text{ et } \Delta H = -553 \cdot 10^3 \text{ J} \cdot \text{mol}^{-1}$$

The reaction system was homogeneous and incompressible. Mass and energy balances were established by using the following assumptions:

- Fluids were not in laminar flow since the Reynolds number was found to be higher than 4000.
- Temperature radial variation was neglected since the Peclet number in our experiments was higher than 1.
- Thermophysical properties of the fluid in the temperature range studied were assumed to be constant.
- Heat transfer with external environment was neglected, because the reactor is isolated
- Spontaneous hydrogen peroxide decomposition in the temperature rang studied was not considered.

To obtain the governing differential equations at steady state, the tubular reactor was subdivided into many elemental volumes of length dx . Simplification and rearrangement of the mass balance equations and energy balance equations led to system (3). In the second equation of system (3), the symbol \pm distinguishes the co-current from the counter current flow configuration. The different parameters of system (3) are defined in nomenclature. More detail on the calculation of the global heat transfer coefficient U is given in (Vernières-Hassimi, 2006). The boundary conditions are the inlet temperature of the reactant mixture, inlet temperature of the coolant, and inlet concentrations of the reactants designated by: For co-current cooling: $T_r(0)=T_{r,in}$, $C_A(0)=C_{A,in}$, $C_B(0)=C_{B,in}$ et $T_c(0)=T_{c,in}$. For counter-current cooling: $T_r(0)=T_{r,in}$, $C_A(0)=C_{A,in}$, $C_B(0)=C_{B,in}$ et $T_c(L)=T_{c,in}$. To solve System (3), the iterative McCormack method was used in a Matlab® environment (McCormack, 1971). The model has been validated in previous work of our group (Vernières-Hassimi et al. 2015).

$$\left\{ \begin{array}{l} \frac{dT_r(x)}{dx} = \frac{K_r}{V_r} (T_c(x) - T_r(x)) - \frac{\Delta H}{V_r \rho_r C_{pr}} A_0 \exp\left(\frac{-E}{RT_r(x)}\right) C_A^\alpha(x) C_B^\beta(x) \\ \frac{dT_c(x)}{dx} = \pm \frac{K_c}{V_c} (T_r(x) - T_c(x)) \\ \frac{dC_A(x)}{dx} = \frac{v_A A_0}{V_r} \exp\left(\frac{-E}{RT_r(x)}\right) C_A^\alpha(x) C_B^\beta(x) \\ \frac{dC_B(x)}{dx} = \frac{v_B A_0}{V_r} \exp\left(\frac{-E}{RT_r(x)}\right) C_A^\alpha(x) C_B^\beta(x) \end{array} \right. \quad (3)$$

$$\text{With } K_r = \frac{4U}{\rho_r D_r C_{pr}} \quad \text{and} \quad K_c = \frac{4U D_r}{\rho_c C_{pc} (D_c)^2 - (D_r + 2e_w)^2}$$

In this paper, we present two examples to show that the established model can fit the experimental data for the two cooling configuration.

Counter-current flow configuration

In the counter-current flow configuration, the reactants inlet is at position $x = 0$ m, and the coolant inlet is at position $x = 8.6$ m. Figure 2 (A) shows the experimental and simulated profiles of the reaction mixture temperature and the coolant temperature at steady state. One can notice that our model fits the experimental data. The reaction mixture temperature increases due to the heat generated by the exothermic reaction to reach a maximum of 58.5°C . After reaching maximum temperature, the heat transfer to the cooling fluid is dominant hence decreasing the reaction temperature. The coolant temperature increases along the reactor, as a result of heat transfer between the coolant and the reactant mixture through the wall. Figure 2 (B) shows the reactants concentration profiles obtained from the simulation. The reactants concentrations decrease along the reactor until the total consumption of the limiting reactant is reached at 6 m. After that, the reaction does not occur anymore and only heat transfer takes place. In the interval $[0 \text{ m}, 1.5 \text{ m}]$ for which the reactants concentration are at their highest level, the cooling system provides heat to the reaction mixture. This heat transfer causes an increase in the reaction rate.

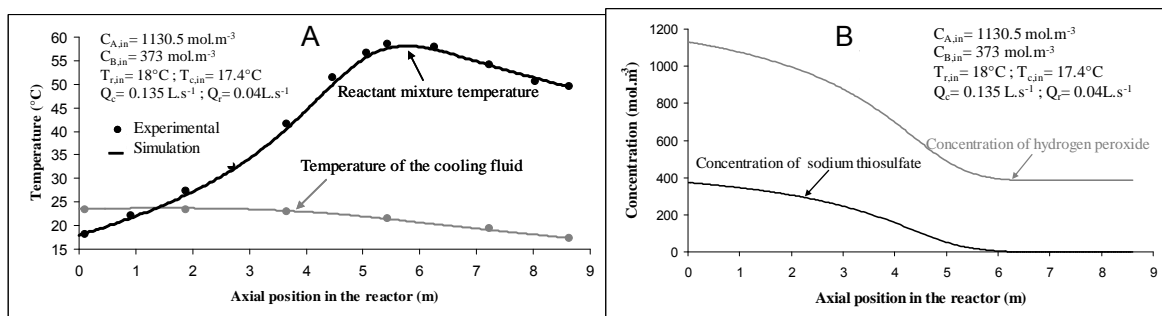


Figure 2: A: Reaction temperature and cooling fluid temperature profiles with counter-current configuration.

B: Simulations profiles of the reactants concentrations with counter-current configuration.

Co-current flow configuration

In the cocurrent flow configuration, the reactants inlet and coolant input are at position $x = 0$ m. Figure 3 (A) shows the experimental and theoretical reactant mixture temperature profiles and the coolant temperature at steady state. One can notice that our model fits the experimental data. The reactant mixture temperature increases due to the heat generated by the exothermic reaction to reach a maximum of 53.7°C . After reaching maximum temperature, the heat transfer with the coolant is dominant decreasing the reaction temperature. The coolant temperature increases along the reactor, as a result of heat transfer between the coolant and the reactant mixture through the wall. Figure 3 (B) shows the reactants concentration profiles. The reactants

concentrations decrease along the reactor until the total consumption of the limiting reactant in the position 7m.

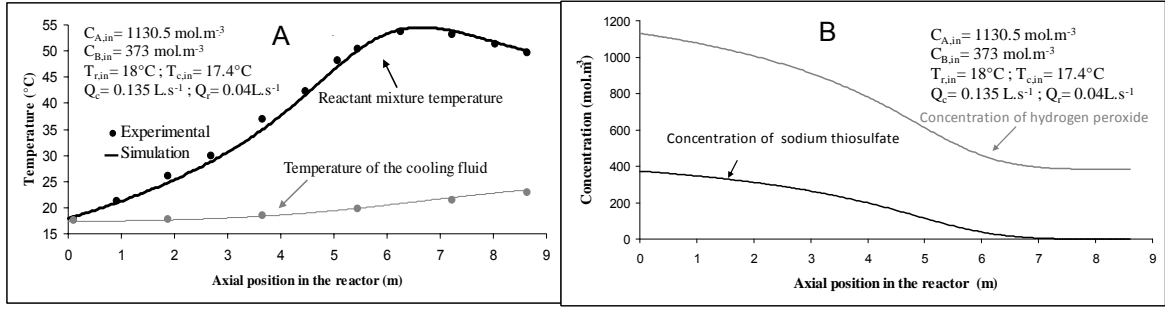


Figure 3:A: Reaction mixture and cooling fluid temperature profiles with co-current flow configuration.
B: Simulations profiles of the reactants concentrations with co-current flow configuration.

4. Results and discussion

In this paragraph, we have studied the parameters that can influence the maximum temperature such as: the coolant volumetric flow rate Q_c , the inlet coolant temperature $T_{c,in}$ and the configuration. Figure 4 (A) shows the influence of the inlet coolant temperature on the maximum reaction temperature. One can notice that for a same value of maximum reaction temperature the inlet coolant temperature for co-current configuration is always lower than for counter-current configuration. This difference is more pronounced for higher maximum temperature. For example, for a maximum temperature of 62°C, the inlet coolant temperature should be of 25°C for a counter-current configuration whereas this temperature should be of 30°C for a co-current configuration. The oxidation of sodium thiosulfate is a fast exothermic reaction, and the reaction temperature reaches its maximum near to the inlet of the reactor. Figure 4(B) shows the influence of the volumetric flow rate of the coolant on the maximum reaction temperature for both configuration. One can notice that for a same value of maximum reaction temperature the volumetric flow rate of coolant Q_c for co-current configuration is always lower than for counter-current configuration. For a maximum reaction temperature of 54°C, the value of Q_c should be of 0.15 L.s⁻¹ for a co-current configuration whereas this value should be of 0.3 L.s⁻¹ for a counter-current configuration. Besides, for a maximum temperature of 54°C and with a coolant volumetric flowrate of 0.15 L.s⁻¹, the value of $T_{c,in}$ should be of 17.4°C for co-current configuration whereas this value should be of $T_{c,in}=15^\circ\text{C}$ for a counter-current configuration.

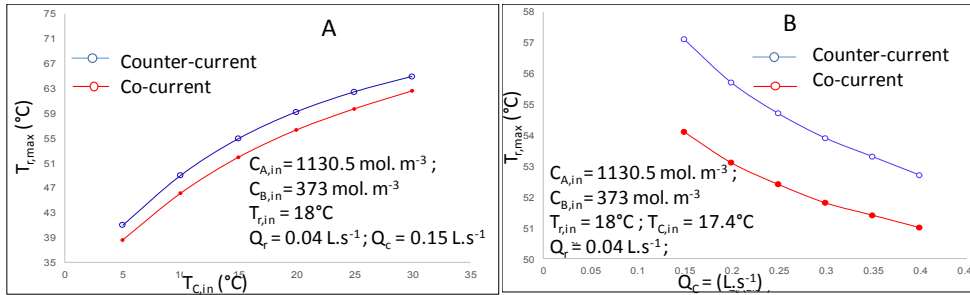


Figure 4: A: Effect of the inlet coolant temperature on the maximum reaction temperature.
B: Effect of the coolant volumetric flow rate on the maximum reaction temperature.

4.1 Analysis of the stability of the tubular reactor

In the present part we apply to our experimental data the criterion formulated by (Dente and Collina, 1964), that historical was the first reactor stability criteria created ad hoc for tubular reactors. According to this criterion, the runaway boundary is defined as a critical condition where the profile of temperature versus axial coordinate exhibited a positive second-order derivative (concave profile) somewhere before the hotspot (i.e. maximum temperature):

$$\frac{d^2\theta}{dz^2} > 0; \frac{d^3\theta}{dz^3} = 0 \quad (4)$$

where θ is the dimensionless temperature of the reactor, defined as per Equation 5:

$$\theta = \frac{T_r - T_{r,in}}{T_{r,in}} \cdot \gamma \quad (5)$$

in which γ is the dimensionless Arrhenius number:

$$\gamma = \frac{E}{R \cdot T_{r,in}} \quad (6)$$

In Figure 5 the results of the sensitivity analysis according to Dente and Collina criterion are shown (in black co-current; in grey counter-current). The results show that counter-current is more unstable: in this configuration, the profile of second order derivative of temperature versus axial coordinate exhibits a higher maximum in comparison to counter current configuration, even if the instability zone seems to be shorter.

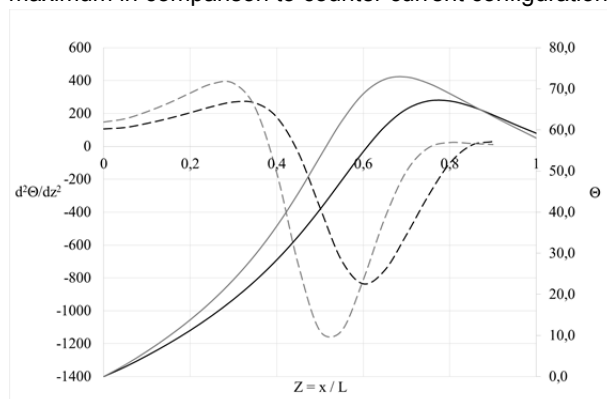


Figure 5: Second order derivative (dotted line, primary axis) of the profile of temperature (solid line, secondary axis) versus axial coordinate ($Z=x/L$) for the case of co-current flow. In black co-current ; in grey counter current.

5. Conclusions

This paper has explored the influence of the cooling configuration on temperature profile in a pilot tubular reactor by using a fast exothermic chemical reaction, i.e., oxidation of sodium thiosulfate by hydrogen peroxide. A mathematical model was built for the two studied configurations: co-current and counter-current cooling systems. The model fitted the experimental data. Based on this model, the influence of the inlet temperature and coolant volumetric flow rate was studied. It was demonstrated clearly that in case of fast exothermic chemical reaction, the co-current configuration should be used to diminish the reaction temperature. The results confirm previous authors observation for which counter-current is more unstable: in this configuration, the profile of second order derivative of temperature versus axial coordinate exhibits a higher maximum in comparison to counter current configuration, even if the instability zone seems to be shorter. This study can be used in order to prevent major accidents.

Acknowledgments

The authors thank also the PHC program Galileo (37267VC).

Nomenclature

| | |
|------------|---|
| A_0 | Frequency factor |
| C | Concentration (mol/m^3) |
| C_p | Specific heat ($\text{J}/\text{kg}\cdot\text{K}$) |
| D | Diameter (m) |
| e_w | Thickness (m) |
| E | Activation energy (J/mol) |
| ΔH | Reaction enthalpy (J/mol) |
| L | length of the reactor (m) |
| r | Reaction rate ($\text{mol}/\text{m}^3\cdot\text{s}$) |
| R | Perfect gas constant ($\text{J}/\text{mol}\cdot\text{K}$) |
| Re | Reynolds number |
| T | Temperature ($^{\circ}\text{C}$) |
| V | Mean velocity (m/s) |
| x | Axial position (m) |
| U | Global heat transfer coefficient ($\text{W}/\text{m}^2\cdot\text{K}$) |

Greek symbol

| | |
|-----------|---|
| α | Reaction parameter |
| β | Reaction parameter |
| λ | Thermal conductivity ($\text{W}/\text{m}\cdot\text{K}$) |

ν Stoichiometric coefficient
 ρ Density (kg/m³)

Index

A Hydrogen peroxide
 B Sodium thiosulfate
 c Coolant fluid
 r Reaction medium

References

- Aimé N., Aide à la conduite sûre des réacteurs chimiques semi-continus en marche normale ou incidentielle vis-à-vis du danger d'emballement, (1991), Doctoral thesis at Université de Technologie de Compiègne, France.
- Brungs M.P., Madden B.G., Seage P.L., 1988, Simulation and experimental studies of metastable states of peroxide reactions in stirred reactors, *Chem. Eng. Sci.* 43 2451–2455. doi:10.1016/0009-2509(88)85179-0.
- Casson V., Snee T., Maschio G., 2014, Investigation of an accident in a resins manufacturing site: The role of accelerator on polymerisation of methyl methacrylate, *J. Hazard. Mater.* 270 45–52. doi:10.1016/j.jhazmat.2014.01.038.
- Cohen W.C., Spencer J.L., 1962, Determination of chemical kinetics by calorimetry, *Chem. Eng. Prog.* 58(2) 40-44.
- Copelli, S., 2016. Chemical Reactors Safety, *Chem, Mol. Sci. and Chem. Eng.* 1–34. doi:10.1016/B978-0-12-409547-2.11115-1
- Dakkoune A., Vernières-Hassimi L., Leveneur S., Lefebvre D., Estel L., 2018, Risk analysis of French chemical industry, *Saf. Sci.* 105, 77-85
- De Morais E.R., Vasco de Toledo E.C., Maciel Filho R., Wolf Maciel M.R., 2004, Alternative Designs for Fixed Bed Catalytic Reactors, *I. J. C. R. E.* 2. doi:10.2202/1542-6580.1181.
- Dente M., Collina A., 1964, Sensitivity behavior of tubular chemical reactors *Chimica Ind.* 46, pp. 752-761.
- Grau M.D., J.M. Nogués J.M., Puigjaner L., 2002, Comparative study of two chemical reactions with different behaviour in batch and semibatch reactors, *Chem. Eng. J.* 88 225–232.
- Guo Z.C., Bai W.S., Chen Y.J., Wang R., Hao L., Wei H.Y., 2016, An adiabatic criterion for runaway detection in semibatch reactors, *Chem. Eng. J.* 288 50–58.
- Leveneur S., Vernières-Hassimi L., Salmi T., 2016, Mass & energy balances coupling in chemical reactors for a better understanding of thermal safety, *Educ. Chem. Eng.* 16, 17–28. doi:10.1016/j.ece.2016.06.002.
- Lo S.N., Cholette A., 1972, Experimental study on the optimum performance of an adiabatic MT reactor, *Can. J. Chem. Eng.* 50 71–80. doi:10.1002/cjce.5450500113.
- Luss, D., Medellin, P., 1972, Steady State Multiplicity and Stability in a Countercurrently Cooled Tubular Reactor, in: *Proceedings of the Fifth European/Second International*
- MacCormack R.W., 1971, Numerical solution of the interaction of a shock wave with a laminar boundary layer, in: M. Holt (Ed.), *Proceedings of the Second International Conference on Numerical Methods in Fluid Dynamics*, Springer Berlin Heidelberg, Berlin, Heidelberg,: pp. 151–163. doi:10.1007/3-540-05407-3_24.
- Maestri F., Rota R., 2006, Temperature diagrams for preventing decomposition or side reactions in liquid–liquid semibatch reactors, *Chem. Eng. Sci.* 61 3068–3078. doi:10.1016/j.ces.2005.11.055.
- Saada R., Patel D., Saha B., 2015, Causes and consequences of thermal runaway incidents—Will they ever be avoided?, *Process. Saf. Environ. Prot.* 97, 109–115. doi:10.1016/j.psep.2015.02.005.
- Torré J.-P., Fletcher D.F., Lasuye T., Xuereb C., 2008, An experimental and CFD study of liquid jet injection into a partially baffled mixing vessel: A contribution to process safety by improving the quenching of runaway reactions, *Chem. Eng. Sci.* 63 924–942. doi:10.1016/j.ces.2007.10.031.
- Vernières-Hassimi L., Estimation et localisation stationnaire et instationnaire de la température maximale pour la sécurité d'un réacteur chimique exothermique tubulaire, (2006), Doctoral thesis at Université Rouen, France.
- Vernières-Hassimi L., Leveneur S., 2015, Alternative method to prevent thermal runaway in case of error on operating conditions continuous reactor, *Process. Saf. Environ. Prot.* 98 365–373. doi:10.1016/j.psep.2015.09.012.
- Vernières-Hassimi L., Seguin D., Abdelghani-Idrissi M.A., Mouhab N., 2015, Estimation and Localization of Maximum Temperature in a Tubular Chemical Reactor by Luenberger State Observer, *Chem. Eng. Com.* 202 70–77. doi:10.1080/00986445.2013.828609.
- Westerterp K.R., Molga E.J., 2006, Safety and Runaway Prevention in Batch and Semibatch Reactors—A Review, *Chem. Eng. Res. Des.*, 84 543–552. doi:10.1205/cherd.05221.